Asymmetric Binding of Stigmatellin to the Dimeric *Paracoccus denitrificans* bc_1 Complex

EVIDENCE FOR ANTI-COOPERATIVE UBIQUINOL OXIDATION AND COMMUNICATION BETWEEN CENTER P UBIQUINOL OXIDATION SITES*[S]

Raul Covian[‡], Thomas Kleinschroth[§], Bernd Ludwig[§], and Bernard L. Trumpower[‡1]

From the [‡]Department of Biochemistry, Dartmouth Medical School, Hanover, New Hampshire 03755 and the [§]Institut für Biochemie, Johann Wolfgang Goethe-Universität and Cluster of Excellence Macromolecular Complexes 60439, Frankfurt, Germany

We have investigated the mechanism responsible for half-of-the-sites activity in the dimeric cytochrome bc_1 complex from *Paracoccus denitrificans* by characterizing the kinetics of inhibitor binding to the ubiquinol oxidation site at center P. Both myxothiazol and stigmatellin induced a 2–3 nm shift of the visible absorbance spectrum of the b_L heme. The shift generated by myxothiazol was symmetric, with monophasic kinetics that indicate equal binding of this inhibitor to both center P sites. In contrast, stigmatellin generated an asymmetric shift in the b_L spectrum, with biphasic kinetics in which each phase contributed approximately half of the total magnitude of the spectral change. The faster binding phase corresponded to a more symmetrical shift of the b_L spectrum relative to the slower binding phase, indicating that approximately half of the center P sites bound stigmatellin more slowly and in a different position relative to the b_L heme, generating a different effect on its electronic environment. Significantly, the slow stigmatellin binding phase was lost as the inhibitor concentration was increased. This implies that a conformational change is transmitted from one center P site in the dimer to the other upon stigmatellin binding to one monomer, rendering the second site less accessible to the inhibitor. Because the position that stigmatellin occupies at center P is considered to be analogous to that of the quinol substrate at the moment of electron transfer, these results indicate that the productive enzyme-substrate configuration is prevented from occurring in both monomers simultaneously.

The cytochrome bc_1 complex is a multisubunit enzyme commonly found in mitochondrial and bacterial membranes. Electron transfer from QH_2[2] to cytochrome c is achieved with three subunits of the complex, cytochrome b, the Rieske iron-sulfur protein, and cytochrome c_1, which are the only subunits in the bc_1 complex from bacteria such as *Paracoccus denitrificans* (1). Both the 3-subunit bacterial bc_1 complex (2) as well as the more complicated 9- to 11-subunit eukaryotic enzymes (3–5) exist as dimeric structures. The intertwined arrangement of the two Rieske proteins, which shuttle electrons from QH_2 oxidation at center P to cytochrome c_1 in each monomer, prevents the dissociation of the dimer without the complete loss of function. Therefore, the conserved dimeric structure seems to have been selected very early in evolution to allow electron transfer in two tightly associated monomeric units.

In previous studies using the yeast bc_1 complex, we have provided evidence that only one center P site oxidizes QH_2 at a time (6) and that electrons equilibrate rapidly between cytochrome b subunits via the b_L hemes (7), highlighting the functional relevance of the dimeric structure. More recently, we have found that the two Q reduction (center N) sites in the dimer exhibit different kinetic properties with respect to each other when both Rieske proteins are located close to center P (8). These results imply conformational communication between center P and center N, as well as between center N sites. We have proposed that all these features of the dimer allow electrons from center P to be more easily recycled back to Q at center N, thereby preventing electrons from accumulating in cytochrome b, which could potentially cause electron leakage to oxygen (7, 8).

An important prediction of an alternating half-of-the-sites activity model for the dimeric bc_1 complex is that each center P site should be able to sense and respond to the conformation and occupancy state of the other. In this work, we have taken advantage of the strong spectral shift induced by the tight binding of the center P inhibitors myxothiazol and stigmatellin to the *P. denitrificans* cytochrome bc_1 complex to reveal conformational communication between center P sites. Our results support a mechanism in which induction of the catalytically competent conformation at one center P upon ligand binding transmits a conformational change to the other monomer, preventing QH_2 oxidation by the second center P site.

EXPERIMENTAL PROCEDURES

Materials—Dodecylmaltoside was obtained from Anatrace. Stigmatellin, myxothiazol, and decylbenzoquinone were purchased from Sigma, DBH_2 was prepared from decylbenzoqui-

---

[S] The on-line version of this article (available at http://www.jbc.org) contains supplemental Fig. S1 and additional text.

[1] To whom correspondence should be addressed: Dept. of Biochemistry, Dartmouth Medical School, 7200 Vail, Hanover, NH 03755. Tel.: 603-650-1621; Fax: 603-650-1128; E-mail: Trumpower@Dartmouth.edu.

[2] The abbreviations used are: QH_2, quinol; DBH_2, decylubiquinol (2,3-dimethoxy-5-methyl-6-decyl-1,4-benzoquinol); UHDBT, 5-*n*-undecyl-6-hydroxy-4,7-dioxobenzothiazole; MES, 4-morpholineethanesulfonic acid.

JOURNAL OF BIOLOGICAL CHEMISTRY **22289**

none (9). All inhibitors as well as DBH_2 were quantified by UV-spectroscopy (10) using reported extinction coefficients (11, 12).

Mutagenesis and Purification of Cytochrome bc₁ Complex— The Y159F mutation was introduced with the Altered Sites system (Promega, Madison, WI) as described previously (13). The *fbc* operon encoding the wild-type or the mutated *P. denitrificans bc₁* complex was cloned into the HindIII/SacI sites of the vector pRI2 (14). The resulting plasmids were conjugated into a chromosomal *fbc* deletion mutant of *P. denitrificans* (15) resulting in strains overexpressing the enzyme. Cell growth, membrane isolation, solubilization, and subsequent protein purification were performed essentially as described before (13), with some modifications. Membranes were solubilized with dodecylmaltoside (1.2 g/g of protein) and diluted to a salt concentration of 350 mM NaCl with 50 mM MES/NaOH (pH 6.0), 0.02% (w/v) dodecylmaltoside before anion exchange chromatography. A salt gradient between 350 and 600 mM NaCl in the above detergent buffer was applied. The *bc₁* enzyme eluted around 450 mM NaCl, and pooled fractions were concentrated by ultrafiltration (Amicon Centricon, exclusion limit 100 kDa), applied to a gel-filtration column (Superose 6 prep grade), equilibrated with the same buffer as mentioned above, and concentrated again to a final *bc₁* enzyme concentration of ~0.1–0.3 mM.

The complex was identified and checked for its quality by SDS-PAGE, Western blotting, redox spectra, and activity measurement, giving the same results as published earlier (13). Extinction coefficients used for quantification of the purified complex were 23.2 mM^{-1} cm^{-1} for cytochrome c_1 at 553–539 nm based on the pyridine hemochrome spectrum (16), and 25.6 mM^{-1} cm^{-1} at 561- 578 nm for cytochrome *b* as reported for other organisms (17). Use of these extinction coefficients yielded a $b{:}c_1$ hemes ratio of 2.0.

Pre-steady State Reduction of bc₁ Complex or Exogenous Cytochrome c—Pre-steady state reduction of cytochrome c_1, cytochrome *b*, and exogenous horse heart cytochrome *c* was followed at room temperature by stopped-flow rapid scanning spectroscopy using the OLIS rapid scanning monochromator as described before (6, 18). For these experiments, we used a *bc₁* complex with a Y159F mutation in the Rieske protein, which has a ~44 mV lower E_m value for the Rieske iron-sulfur cluster than in the wild-type enzyme (13), favoring electron distribution into cytochrome c_1. Reactions were started by rapid mixing of 2.2 µM enzyme with or without 15 µM horse heart cytochrome *c* in assay buffer containing 50 mM potassium phosphate, pH 7.5, 2 mM sodium azide, 0.2 mM EDTA, and 0.05% dodecylmaltoside against an equal volume of the same buffer containing 24 µM DBH_2. In some experiments, 2.5 µM antimycin was added to the enzyme mixture 2 min before rapid mixing. For each experiment, 12–15 datasets were averaged after subtracting the oxidized spectrum. The time course of absorbance change at the appropriate wavelengths was extracted using software from OLIS and exported to the Origin 5.0 program (OriginLab Corp.). The contribution of cytochrome *b* to c_1 absorbance was calculated and corrected for as previously described (6). Absorbance changes as a function of time were fitted to monophasic or biphasic expo-

nential functions in Origin. When present, cytochrome *c* reduction was quantified using an extinction coefficient of 21.5 mM^{-1} cm^{-1} (19).

Kinetic Modeling—Cytochrome c_1 and cytochrome *c* reduction were fitted or simulated using the Dynafit program (Biokin Ltd.), which allows the comparison of time-dependent data to different reaction mechanisms described as a series of kinetic steps (20). The script files describing the mechanisms are provided as supplemental material and are similar to those we have reported for the yeast bc₁ complex (6), with variations accounting for the particular E_m values of the *P. denitrificans* enzyme. Individual rate constants were fixed to non-rate-limiting values, and only the substrate binding rate constant was allowed to vary during fitting. The forward rate of DBH_2 oxidation was fixed to 48 s^{-1}, the turnover rate of the Y159F enzyme under steady-state conditions.

The E_m values at pH 7.5 of each redox group were used to set the ratios of forward and reverse rates at each electron transfer step. For DBH_2, a value of 60.5 mV was assumed considering a ΔE_m of 59 mV/pH unit from E_{m7} = 90 mV. The Y159F mutant Rieske protein was assumed to have a E_m of 221 mV based on a ΔE_m of −44 mV with respect to the 265-mV value reported for the wild type (13, 21). The lowest in the range of E_m values reported for the *P. denitrificans* cytochrome c_1 (22) was used (268 mV). E_m values for heme b_H and b_L were assumed to be +58 and −92 mV, respectively (22). Using the Nernst equation, the ΔE_m of 79 mV between DBH_2 and the average E_m for the Rieske protein and the b_H heme (139.5 mV) was used to set a forward/reverse rate ratio of 4.7 for the first turnover at center P. For the second turnover, an average E_m of 64.5 mV for the Rieske protein and the b_L heme was used to set a rates ratio of 1.08. Electron transfer from the Rieske protein to cytochrome c_1 was assumed to be favored by a factor of 2.33 over the reverse process based on a ΔE_m of 47 mV.

For modeling of exogenous cytochrome *c* reduction, electron transfer from c_1 was assumed to occur with K_{eq} = 1. The antimycin-insensitive reduction of cytochrome *c* mediated by superoxide formation was expressed as a single step in which oxygen binding to the QH_2-occupied center P resulted in superoxide formation and Rieske protein reduction with a rate that was adjusted during the fitting. Superoxide was then assumed to reduce cytochrome *c* directly with a bimolecular rate of 1.1 × 10^6 M^{-1} s^{-1} (23).

Kinetics of Inhibitor Binding to the bc₁ Complex—Purified *bc₁* complex from wild-type *P. denitrificans* was diluted to 4 µM in the same buffer used for pre-steady state experiments, reduced with dithionite, and mixed rapidly against an equal volume containing the indicated concentration of myxothiazol or stigmatellin. The fully reduced spectrum before mixing was stored as a baseline and subtracted from all subsequent scans, 10–12 datasets were averaged, and the time course of absorbance change at selected wavelengths was exported to the Origin program. The differences in absorbance between the peak, trough, and isosbestic point of the spectral shifts induced by inhibitor binding were plotted and fitted to monophasic or biphasic exponential functions.
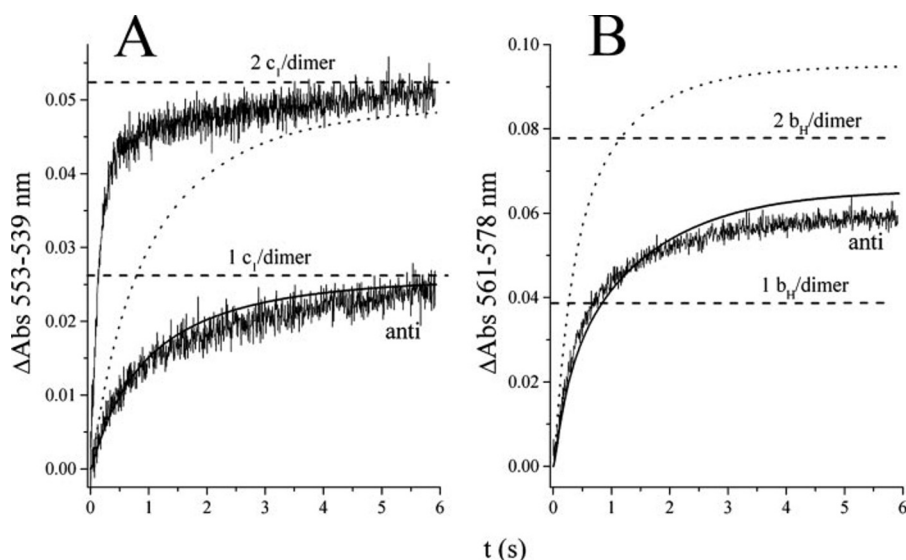
FIGURE 1. **Pre-steady state reduction of the *P. denitrificans* bc$_1$ complex with the Y159F mutation in the Rieske protein.** Cytochrome c_1 (*A*) and cytochrome *b* (*B*) reduction by 24 μM DBH$_2$ was determined in the presence or absence of 1.1 equivalents of antimycin per *bc$_1$* monomer. The *solid curves* represents the fitting to a Dynafit model (see supplemental material for details) assuming only half of the center P sites are active when antimycin is present, and allowing electron equilibration between cytochrome *b* subunits in the dimer. The *dotted curves* represent a simulation using the same kinetic constants derived from the fitting, but assuming that all center P sites are able to oxidize DBH$_2$. The enzyme monomer concentration was 1.1 μM. The absorbance changes corresponding to 1 or 2 equivalents of c_1 (in *A*) or b_H (in *B*) per dimer are indicated by *horizontal dashed lines*.
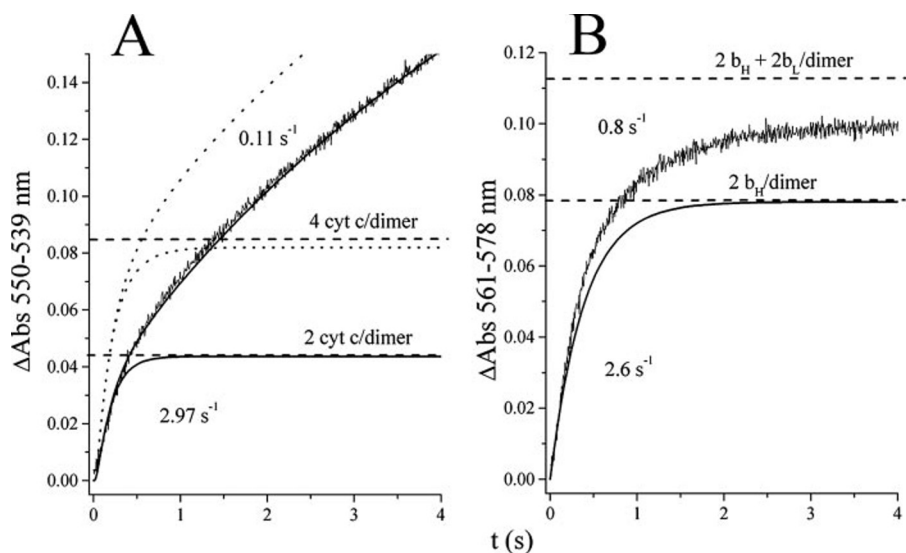

FIGURE 2. **Pre-steady state reduction by the *P. denitrificans* Y159F bc$_1$ complex in the presence of exogenous cytochrome c.** Reduction of cytochrome *c* (*A*) and cytochrome *b* (*B*) by 24 μM DBH$_2$ was determined in the presence of 1.1 equivalents of antimycin per *bc$_1$* monomer. The *solid line* close to the experimental kinetic trace in *A* represents the fitting to a Dynafit model (see Supplemental Data for details) assuming only half of the center P sites are active. The solid curve that becomes asymptotic at 2 cytochrome *c* per dimer corresponds to that same fitted curve without the second slow phase of cytochrome *c* reduction. Dotted curves are simulations using the same kinetic constants as in the fitting, but assuming that all center P sites are active, with or without the second slow reduction of cytochrome *c*. The *solid line* in *B* corresponds to the fast phase of cytochrome *b* reduction only, calculated from fitting the kinetic trace to a second order exponential function.

RESULTS

Half-of-the-sites Reactivity at Center P in the Presence of Antimycin—The pre-steady state reduction of the *P. denitrificans bc$_1$* complex containing the Rieske protein with the Y159F mutation is shown in Fig. 1. Both cytochrome c_1 subunits in the dimer underwent almost complete reduction in the uninhibited condition, but only half were reduced in the presence of anti-

mycin (Fig. 1*A*). Because the Rieske iron-sulfur cluster in this mutant has an E_m that is 44 mV lower than that of the c_1 heme (13), a 70% reduction of cytochrome c_1 should have occurred after the first turnover at center P, assuming all monomers were active. Moreover, with the assumption that each monomer functions independently, the kinetic modeling showed that a partial second turnover should be expected even if the b_H heme in each monomer is inaccessible as electron acceptor due to antimycin inhibition of b_H heme reoxidation, yielding a final extent of c_1 reduction of 90% (*dotted line*, Fig. 1*A*). In contrast, if only one center P per dimer was assumed to be active and electron crossover between monomers occurs, the resulting predicted curve (*solid line*) corresponded closely with the experimentally observed cytochrome c_1 reduction of ~45%.

Cytochrome *b* reduction kinetics in the presence of antimycin (Fig. 1*B*) also agreed with the interpretation that only one center P was active. Kinetic modeling showed that both b_H hemes in the dimer plus a fraction of the b_L hemes should have undergone reduction if DBH$_2$ oxidation had occurred at center P in both monomers (*dotted line*). Assuming only one monomer was active resulted in a much better fit to the observed extent of reduction (*solid curve*). This model assumed that the electron from a second turnover at the only active center P in the dimer could reach the b_H heme in the inactive monomer, resulting in ~80% reduction of both b_H hemes.

Pre-steady state reduction kinetics in the presence of exogenously added cytochrome *c* and antimycin are shown in Fig. 2. Within 1 s, ~2 cytochrome *c* molecules (Fig. 2*A*) and 2 b_H hemes (Fig. 2*B*) per dimer underwent reduction in a fast phase. This was followed by a slower phase during which several equivalents of cytochrome *c* were reduced with only a part of the b_L hemes being reduced at the same time. This slower reduction of cytochrome *c* without a corresponding transfer of electrons to cytochrome *b* was evidently due to the leakage of one of the electrons derived from DBH$_2$ oxidation at
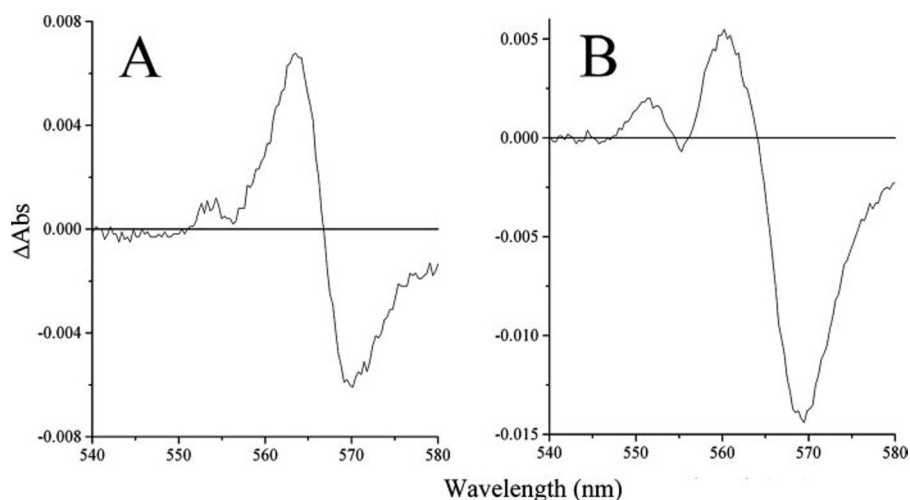
FIGURE 3. **Spectral shifts induced by center P inhibitors in the absorbance of the reduced *P. denitrificans* bc₁ complex.** Purified wild-type enzyme (2 μM, expressed as monomers) was mixed with 40 μM myxothiazol (*A*) or stigmatellin (*B*) after reduction with dithionite. Spectra of the reduced enzyme were collected 2 min after addition of inhibitor and subtraction of the scans collected before mixing.

center P to oxygen to form superoxide, which can itself reduce cytochrome *c* (24, 25). We confirmed that superoxide formation was involved in this slow cytochrome *c* reduction by performing the assay in the presence of manganese-superoxide dismutase, which resulted in the expected 40–50% inhibition in the rate of the second phase of cytochrome *c* reduction (results not shown).

The first fast phase of simultaneous *c* and b_H reduction was used to determine how many center P sites were active per dimer. Kinetic modeling showed that the reduction of almost 4 cytochrome *c* equivalents per dimer should have occurred in the fast phase (which corresponds to the bifurcated DBH₂ oxidation) if all center P sites had been active (*dotted curves* in Fig. 2*A*), corresponding to two turnovers per monomer. This expectation comes from the equilibrium constants for the first and second turnovers at each active center P in the antimycin-inhibited enzyme, which were set to 4.7 and 1.08, respectively (see "Experimental Procedures" and supplemental material). Given that both DBH₂ and cytochrome *c* were present in super-stoichiometric concentrations with respect to the enzyme, almost two full turnovers per active center P are thermodynamically possible. Therefore, a good fit of the experimental data was obtained only if one center P site per dimer was considered to be active (*solid curves*), corresponding to the reduction of 2 cytochrome *c* equivalents per dimer during the fast kinetic phase.

Heme b_L Spectral Shifts Induced by Binding of Center P Inhibitors—The fully reduced *P. denitrificans bc₁* complex exhibits a shoulder at 566 nm, which corresponds to the absorbance maximum of the b_L heme (1). As shown in Fig. 3, when this reduced spectrum is taken as a baseline and myxothiazol or stigmatellin are added to the *P. denitrificans* enzyme, the maximal absorbance of the b_L heme shifts 2 or 3 nm, respectively, to a lower wavelength. As can be seen in Fig. 3*A*, the peak generated by myxothiazol at 563 nm was mirrored by a trough of equivalent amplitude at 569 nm. The symmetry of this spectral shift implies that the shape of the b_L absorbance spectrum was not altered, suggesting a homogeneous binding

of myxothiazol to all center P sites. This inhibitor binds to a sub-domain within center P that is located proximal to the b_L heme and does not establish any interactions with the Rieske protein (4). Another inhibitor that binds to the same pocket is methoxyacrylate stilbene (26). This inhibitor also generated a symmetrical shift, with a peak equal in magnitude to the trough, in the spectrum of the b_L heme (result not shown), although the peak was shifted to a longer wavelength (568 nm) instead of to a shorter one (563 nm), as was the case with myxothiazol.

As shown in Fig. 3*B*, binding of stigmatellin changed not only the wavelength of maximal b_L heme absorbance, but also the shape of the resulting difference spectrum. This was evidenced as a trough at 569 nm that was ~3-fold larger in amplitude than the peak at 562 nm, due to a pronounced narrowing of the b_L spectrum at higher wavelengths (565–569 nm). This result indicates either heterogeneous binding of stigmatellin to a fraction of center P sites, or alternatively, a decrease in the extinction coefficient of the b_L heme along with a spectral shift upon homogeneous binding of the inhibitor. Stigmatellin binds to a center P sub-domain different than the one to which myxothiazol binds, being at a greater distance from the b_L heme and establishing a hydrogen bond with a histidine residue that is coordinated to the FeS cluster of the Rieske protein (4). UHDBT is another inhibitor that binds to the same pocket as stigmatellin, although more weakly (11, 26). UHDBT also generated an asymmetrical blue shift in the absorbance spectrum of the b_L heme, although its magnitude was only ~25% of that induced by stigmatellin (not shown).

Binding Kinetics of Myxothiazol to Center P—The symmetrical blue shift of b_L absorbance generated by myxothiazol was followed as a function of time to determine the binding rate of this inhibitor to center P, as shown in Fig. 4. Myxothiazol bound in a single kinetic phase at all concentrations tested, resulting in a linear relation between binding rate and inhibitor concentration (Fig. 4*B*). The slope of this plot corresponds to the value of the second order rate constant for myxothiazol binding (8.4×10^4 M^{-1} s^{-1}). The value of the intercept with the *y*-axis gives an estimate of the dissociation rate constant and, as expected for a tightly bound inhibitor, was very close to zero (0.04 s^{-1}).

This result indicates that myxothiazol binds with the same kinetics to both center P sites in the *bc₁* complex dimer. The addition of one equivalent of antimycin per *bc₁* monomer before rapid mixing with myxothiazol gave the same kinetic results for myxothiazol binding, although the amplitude of the blue shift was decreased by 50% (data not shown). This indicates that the rate of myxothiazol binding and its symmetry were not affected by the presence of the center N inhibitor, although the position of myxothiazol relative to the b_L heme
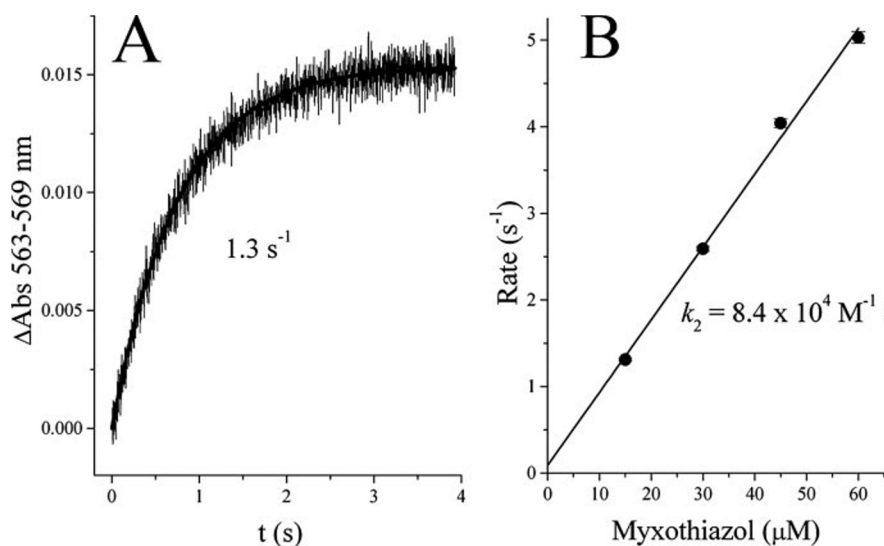
FIGURE 4. **Kinetics of myxothiazol binding to the reduced *P. denitrificans bc$_1$* complex.** *A,* time-dependent increase in the magnitude of the spectral shift generated by binding of 15 μM myxothiazol to 2 μM wild-type enzyme. The *solid curve* represent the fit to a first order exponential function. *B,* binding rates determined at different myxothiazol concentrations. The *solid line* is the fit of the experimental data to a linear function, yielding a slope value corresponding to the second order binding rate constant (k_2).
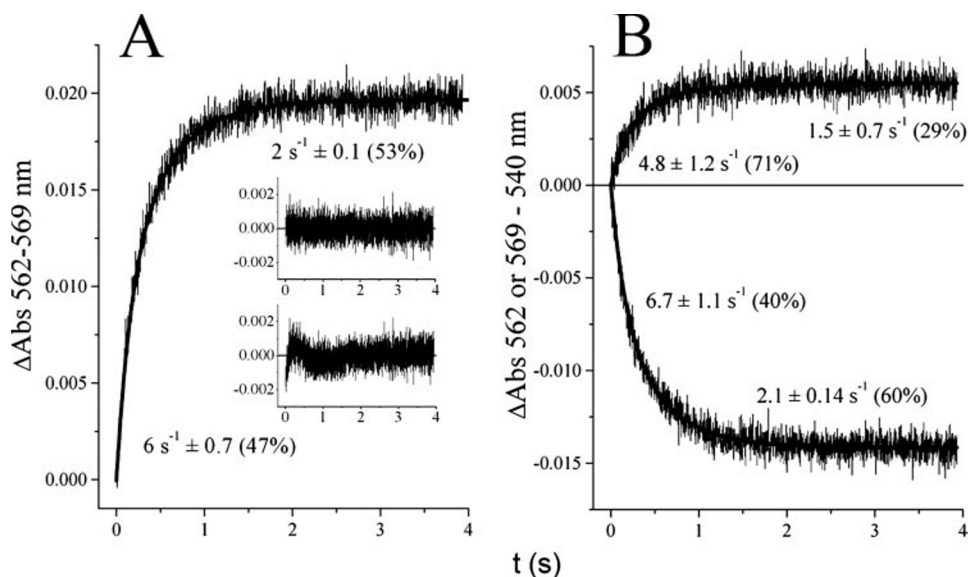

FIGURE 5. **Binding kinetics of 15 μM stigmatellin to the reduced *P. denitrificans bc$_1$* complex.** *A,* time-dependent increase in the magnitude of the spectral shift generated by binding of 15 μM stigmatellin to 2 μM wild-type enzyme. *B,* time-dependent increase or decrease in absorbance of the peak (562 nm) and trough (569 nm) of the spectral shift induced by stigmatellin binding. *Solid curves* are best fits to a second order exponential function. For each *trace,* the relative contribution of each kinetic phase to the absorbance change is shown in parentheses next to its corresponding fitted rate. The *inset* in *A* shows the residual plot resulting from fitting to a biphasic (*top*) or to a monophasic (*bottom*) exponential function. Fitting to the latter equation resulted in a value of 2.9 $\pm$ 0.04 s^{-1} for the rate of stigmatellin binding.

kinetic component. Poor fitting was obtained if only one kinetic component was assumed, as evidenced in a residual plot by the deviation of the fitted curve with respect to the experimental data points (Fig. 5*A, inset*). This biphasic binding pattern was not caused by a change in free inhibitor concentration as the binding occurred, because myxothiazol at the same ratio of inhibitor to enzyme (7.5:1) gave strictly monophasic kinetics (see Fig. 4*A*).

Furthermore, as shown in Fig. 5*B,* each kinetic phase contributed differently to the peak and trough of the spectral blue shift. Thus, when the absorbance at a wavelength where inhibitor binding had no effect on the spectrum (540 nm) was subtracted from the absorbance change at the wavelength of the peak (562 nm), it became evident that the fast kinetic phase was responsible for over two-thirds of the absorbance increase. In contrast, the slow phase accounted for most of the decrease in absorbance at the spectral trough (569 nm). This indicates that (*a*) stigmatellin binding induces a different effect upon b_L heme absorbance at approximately half of the center P sites, and (*b*) the asymmetric spectral shift observed after equilibration with the inhibitor (see Fig. 3*B*) cannot be attributed to a homogeneous binding of stigmatellin to all center P sites resulting in a simultaneous decrease in the extinction coefficient along with a spectral shift of all b_L hemes. Similar results were obtained when both center N sites were occupied by antimycin, or with the Y159F enzyme (not shown).

The asymmetric binding of stigmatellin was evidenced more clearly by deconvoluting the spectral shift induced by each kinetic phase, as shown in Fig. 6. This was accomplished by averaging the spectra collected within the first 100 ms after mixing with stigmatellin, because during this time range the second phase of binding did not contribute significantly to the overall spectral shift. The absorbance of this averaged spectrum, which comprises only the shift induced by the fast binding event, was multiplied by a factor in order to yield an absorbance equivalent to that of 47% of the total spectral shift, as calculated from the fitting in Fig. 5*A.* The resulting spectrum, shown in Fig. 6*A,* was

appeared to be slightly altered, based on the change in amplitude of the spectral shift. Essentially the same results were obtained when myxothiazol binding was determined in the Y159F mutant enzyme used for the pre-steady reduction assays shown in Figs. 1 and 2 (not shown).

Binding Kinetics of Stigmatellin to Center P—As shown in Fig. 5*A,* the asymmetrical shift in the spectrum of the b_L heme upon binding of 15 μM stigmatellin occurred in two phases, each comprising approximately half of the difference between peak and trough. There was a ~3-fold difference in the rate of each
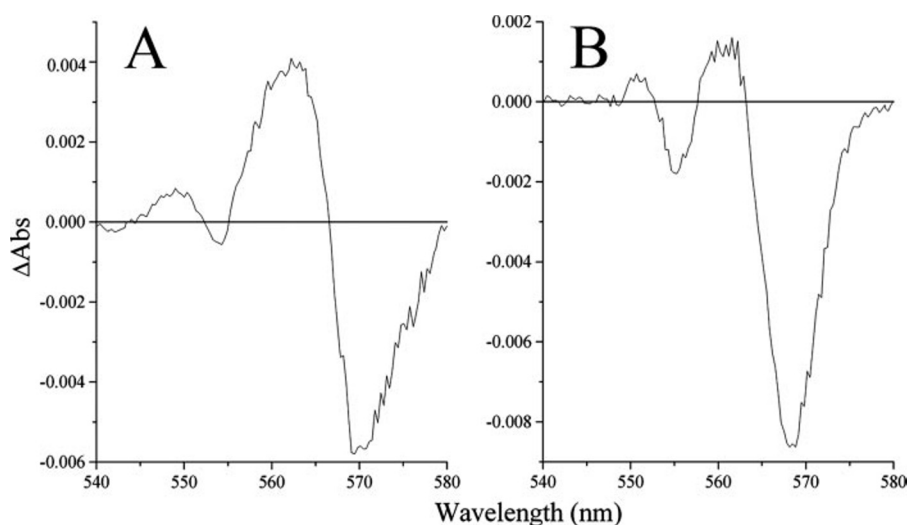
FIGURE 6. **Spectral shift generated by the fast (*A*) and slow (*B*) kinetic phases of stigmatellin binding.** The spectral shift generated by binding of 15 μM stigmatellin to 2 μM *P. denitrificans* wild-type enzyme was deconvoluted into two separate spectra as explained in the text under "Results."

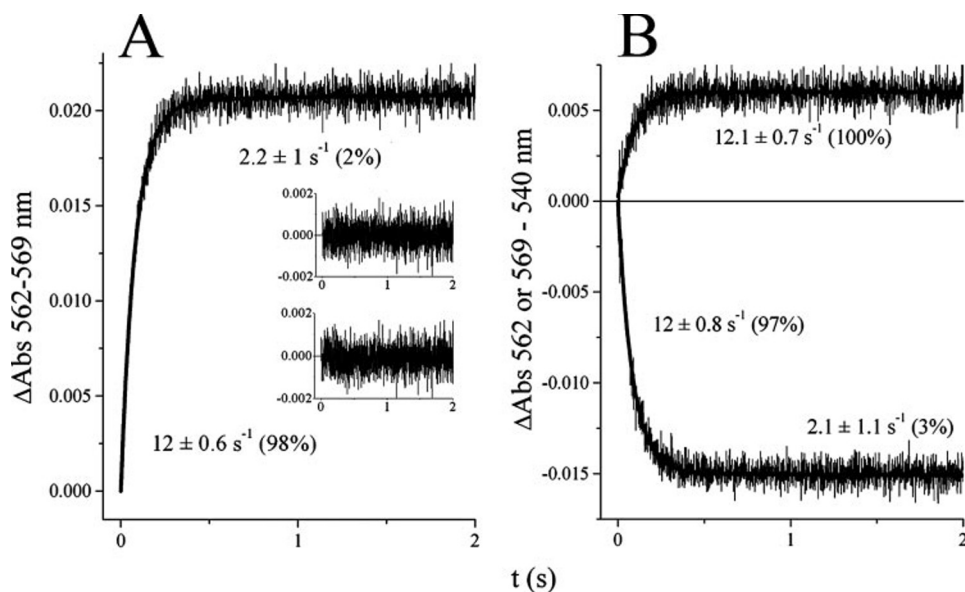FIGURE 7. **Binding kinetics of 60 μM stigmatellin to the reduced *P. denitrificans* bc$_1$ complex.** *A*, time-dependent increase in the magnitude of the spectral shift generated by binding of 60 μM stigmatellin to 2 μM wild-type enzyme. *B*, time-dependent increase or decrease in absorbance of the peak (562 nm) and trough (569 nm) of the spectral shift induced by stigmatellin binding. *Solid curves* are best fits to a first or second order exponential function. For each *trace*, the relative contribution of each kinetic phase to the absorbance change is shown in *parentheses* next to its corresponding fitted rate. The *inset* in *A* shows the residual plot resulting from fitting to a biphasic (*top*) or to a monophasic (*bottom*) exponential function. Fitting to the latter equation resulted in a value of 11.4 $\pm$ 0.2 s^{-1} for the rate of stigmatellin binding.

dimeric *bc$_1$* complex but not with the alternative explanation that the spectral asymmetry is the product of a slow decreased extinction coefficient of the *b$_L$* hemes that occurs after a faster spectral shift generated by homogeneous binding of stigmatellin to all center P sites. The reason for this, as shown in Fig. S1 of the supplemental material, is that a decrease in *b$_L$* extinction coefficient following the generation of an initial symmetric band shift at all center P sites results in a loss of absorbance close to the peak of the shifted *b$_L$* spectrum (562 nm) during the slower kinetic phase, and not at the trough (569 nm), as we observed.

Transition to Monophasic Binding Kinetics at Higher Concentrations of Stigmatellin—In contrast to the biphasic binding kinetics observed at lower inhibitor concentrations, when the *P. denitrificans* enzyme was mixed with 60 μM stigmatellin almost all binding of the inhibitor occurred in a single fast phase as shown in Fig. 7*A*. Because of the small contribution ($\sim$2%) of the second kinetic component to the spectral shift at this concentration of stigmatellin, fitting to first or second order exponential equations resulted in almost undistinguishable curves, although the residual plot revealed a slightly better fit to biphasic kinetics (Fig. 7*A*, *inset*). Surprisingly, the kinetics traces of the peak and trough absorbance changes (Fig. 7*B*) indicate the resulting blue shift was still asymmetric, with the same peak to trough absorbance ratio as was observed at concentrations that presented a biphasic binding pattern. This implies that, although stigmatellin at higher concentrations was able to bind with the same rate to any of the center P sites in the dimer, the position of the inhibitor relative to the *b$_L$* heme was still heterogeneous within the population of center P sites. Thus, the final spectral shift, even when generated in a single fast phase, is an average of two binding modes, one resulting in an almost symmetrical peak like that shown in Fig. 6*A*, and the other that mainly decreases the absorbance at 569 nm, as in Fig. 6*B*. These observations are clearly inconsistent with an equal and independent binding of stigmatellin to both center P sites in the dimer, even if the inhibitor is assumed to

then subtracted from the final spectrum collected at 4 s, when stigmatellin binding was completed. This difference spectrum, shown in Fig. 6*B*, represents the spectral shift induced only by the slow stigmatellin binding phase. As can be seen from these spectra, the initial binding of stigmatellin to one half of the center P sites produced an almost symmetrical blue shift, indicating that the shape and amplitude of the heme spectrum were preserved. In contrast, the remaining half of the absorbance change was observed as a strongly asymmetrical shift composed mainly of a sharp decrease in absorbance centered at 569 nm. Again, this result is consistent with the assumption that stigmatellin binds differently to each of the two center P sites in the
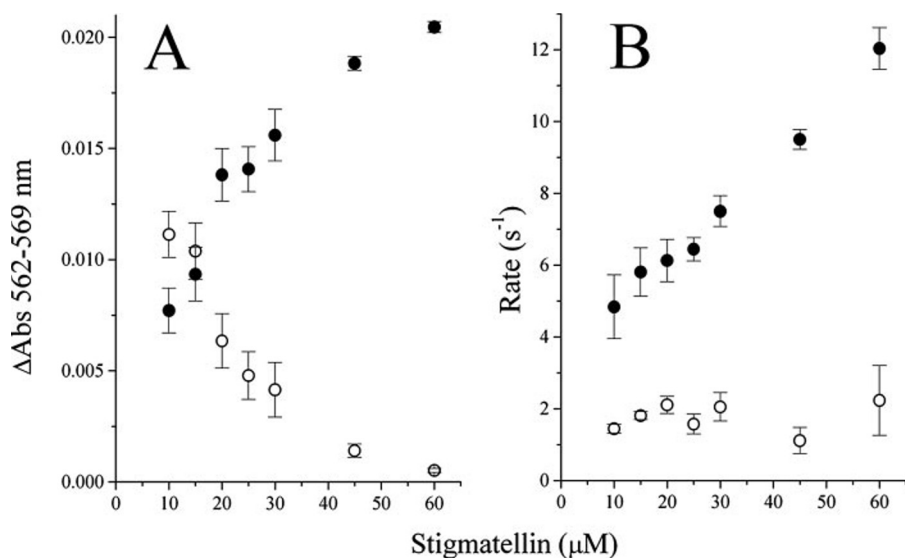
FIGURE 8. **Kinetic properties of the fast and slow phases of stigmatellin binding as a function of inhibitor concentration.** The magnitude of absorbance change (*A*) and the rate (*B*) of the fast (*filled circles*) and slow (*open circles*) kinetic phases of stigmatellin binding are shown at different inhibitor concentrations. Values were obtained by fitting kinetic traces similar to those shown in Figs. 5*A* and 7*A* to a second order exponential function. Enzyme concentration was 2 μM bc_1 monomers in all cases.

generate additional effects once bound, such as a homogeneous decrease in the intrinsic absorbance of all b_L hemes.

The disappearance of the slow kinetic phase of stigmatellin binding occurred gradually as the inhibitor concentration was increased, as shown in Fig. 8. The relative contribution of each phase to the total amplitude of the absorbance change (Fig. 8*A*) was almost equal between 10 and 15 μM stigmatellin, or as long as the rate of the fast binding event remained below 6 s^{-1} (Fig. 8*B*). As the initial binding rate increased upon addition of higher inhibitor concentrations, the contribution of the slow phase to the spectral shift progressively decreased. Interestingly, the rate of the slow binding was not dependent on stigmatellin concentration (Fig. 8*B*), remaining always close to a value of 2 s^{-1}.

The latter observation suggests that the slow binding event is controlled by a conformational change within the dimer that occurs after binding of stigmatellin to the one monomer. Moreover, the fact that binding to the second half of the center P sites begins to escape the control of the first monomer when stigmatellin concentration exceeds 15 μM, which corresponds to a rate >6 s^{-1}, also points to a conformational change transmitted from one monomer to the other. The fast rate of stigmatellin binding remained dependent on inhibitor concentration even at high concentrations of stigmatellin where both center P sites contribute to the binding, although the transition from single site to two site binding deviated slightly from strict linearity (Fig. 8*B*).

DISCUSSION

QH$_2$ oxidation at center P of the bc_1 complex has the unique feature of being a bifurcated electron transfer in which both the Rieske iron-sulfur cluster and the b_L heme each receive an electron. Even though crystal structures have not been able to show the position of QH$_2$ at center P from which electron transfer occurs, it is considered that stigmatellin occupies the same

position as the substrate in the productive enzyme-substrate complex (4, 5). This is due to the fact that the inhibitor forms hydrogen bonds with the Rieske histidine and the cytochrome b glutamate that are the most likely acceptors for the protons accompanying electron transfer from QH$_2$. Stigmatellin binding also immobilizes the extra-membrane domain of the Rieske protein at the interface with cytochrome b. This is the same position that would allow one of the electrons from QH$_2$ at center P to be transferred to the iron-sulfur cluster. Therefore, any mechanism affecting the electron transfer-competent configuration of QH$_2$ and/or the Rieske protein at center P should be expected to modify stigmatellin binding accordingly.

Our present results show that only one center P per dimer is able to oxidize QH$_2$ when antimycin blocks center N reactions in the *P. denitrificans* bc_1 complex, just as we have reported for the yeast enzyme (6). The lower E_m of the Rieske protein in the Y159F mutant that we used in the present study, together with our kinetic modeling using the appropriate equilibria between electron transfer steps, shows that the missing cytochrome c_1 or c absorbance from one half of the monomers cannot be explained by arguing that only one turnover in each monomer occurred, resulting in the electron residing preferentially in the Rieske protein instead of the c_1/c cytochromes. Even if only one turnover is assumed to occur (which does not agree with the K_{eq} for a second turnover, considering the E_m of the b_L heme), 70% of the total c_1 content would undergo reduction, not 50%, as we have observed (see Fig. 1*A*). Furthermore, one turnover at every center P in the presence of antimycin would have resulted in full b_H heme reduction, instead of ~80% (see Fig. 1*B*). Because the presence of super-stoichiometric concentrations of cytochrome c would maintain the Rieske protein and cytochrome c_1 largely oxidized, the interpretation that only one bifurcated QH$_2$ oxidation per center P site can explain the reduction of 2 cytochrome c per dimer together with almost all of the b_H plus b_L hemes (see Fig. 2) is untenable. The only explanation that is consistent with all these results is that QH$_2$ oxidation occurs at only one of the center P sites in the dimer, with electrons being able to equilibrate with the b hemes of the inactive monomer, as happens in the yeast bc_1 complex (6, 7).

We have also taken advantage of the spectral shifts induced by the binding of the center P inhibitors myxothiazol and stigmatellin to the *P. denitrificans* cytochrome bc_1 complex to demonstrate communication between the center P sites. The asymmetric binding of stigmatellin that we have observed in the bacterial enzyme is consistent with the half-of-the-sites activity in the bc_1 complex dimer. It is noteworthy that this inhibitor also produces an asymmetric shift in the bovine bc_1 complex (27, 28), although the displacement of the b_L maximum absorb-

ance in that enzyme is to higher wavelengths (red shift), and not to lower (blue shift) as we presently report in the *P. denitrificans* enzyme (see Fig. 3*B*). The slower binding rate, as well as the different effect that approximately half of the bound stigmatellin exerts on the spectral properties of the b_L heme, indicates that one out of every two monomers positions stigmatellin at center P in a slightly anomalous configuration (see Figs. 5 and 6).

The simplest explanation of the stigmatellin binding results is that the center P binding sites for this inhibitor are non-equivalent environments in the two monomers. Differences between the bc_1 monomers have been revealed by analyzing the orientation of the iron-sulfur cluster EPR g-tensors and the structure of the Rieske-cytochrome *b* interface even when stigmatellin is occupying both center P sites of the bovine bc_1 complex (29). These changes, although subtle, might have dramatic consequences for QH_2 oxidation given the high sensitivity of electron transfer to donor-acceptor distance and the necessity of the hydrogen bond between the substrate and His-155 (181 in yeast) of the Rieske protein (30). The strongly asymmetric b_L spectral shift we have presently found upon addition of stigmatellin is consistent with a slightly modified interaction of the Rieske protein with the cytochrome *b* interface that could result in a different position of the inhibitor relative to the b_L heme.

The stigmatellin binding results that we have observed with the bacterial bc_1 complex are consistent with the kinetic results in the yeast enzyme that point to an anti-cooperative, half-of-the-sites mechanism of QH_2 oxidation (6, 8). We have also now shown that the bacterial enzyme exhibits half-of-the-sites activity at center P (Figs. 1 and 2). Because stigmatellin is a competitive inhibitor of QH_2 oxidation (31), these results suggest that in one center P per dimer the catalytically competent position of QH_2 is impeded whenever the other monomer is in that same productive configuration. There may be an intrinsic difference in stigmatellin affinity due to non-equivalent environments at center P in the two monomers that does not require an anti-cooperative interaction if no ligand is present. However, this would not account for the concentration-independent nature of the slow phase of stigmatellin binding nor its loss at high stigmatellin concentrations. Therefore, we conclude that, under physiological conditions where ubiquinol is present, the bacterial enzyme, like that of yeast, exhibits anti-cooperativity toward the substrate ligand.

This could imply a conformational communication from the active center P that significantly decreases the affinity toward QH_2 in the other site. Alternatively, the substrate could be placed in a slightly different position that prevents electron transfer to the Rieske iron-sulfur cluster in the inactive monomer. The absence of asymmetric or biphasic binding behavior in the case of myxothiazol (see Fig. 4), which does not interact with the Rieske protein, but partially competes with QH_2 (25, 31), supports the notion that substrate-Rieske subunit interaction is involved in the mechanism of anti-cooperative QH_2 oxidation. Significantly, myxothiazol also produces a symmetric shift (although to a higher wavelength) in the absorbance of the b_L heme in the bovine bc_1 complex (27), indicating a homogeneous binding to center P sites in the eukaryotic enzymes.

Another key interaction that could modify the binding kinetics and position of stigmatellin is the hydrogen bond with Glu-295 of cytochrome *b* (272 in eukaryotes). Because this residue is found in different positions depending on the center P ligand (4, 5) and is important both for stigmatellin sensitivity and as an acceptor for one of the protons derived from QH_2 oxidation (32), it seems reasonable to assume that its position could change in the inactive monomer. However, the fact that UHDBT, which immobilizes the Rieske protein but does not depend on Glu-272 for binding (32), also generates an asymmetric shift (data not shown) suggests that a change in the position of Glu-272 is not involved in the different occupancy at the center P sites of the dimer.

The progressive loss of the slow phase of stigmatellin binding at higher concentrations of inhibitor is consistent with a conformational event being transmitted upon binding of the inhibitor to the first monomer, which results in a decreased accessibility at the second center P site. This is also evidenced by the lack of concentration dependence of the slow phase of binding, which remains constant at ~ 2 s^{-1}. This communication pathway between monomers is probably related to the intra-dimeric conformational change we have previously reported at the level of the center N sites (8). In that work, we showed that antimycin binding to center N was biphasic when stigmatellin occupied both center P sites in the yeast dimer, with the slow phase having a concentration independent rate of ~ 2 s^{-1}, the same as the slow phase of stigmatellin binding we have now observed in the *P. denitrificans* enzyme. Therefore, it seems likely that communication between center P sites is transmitted through the center N sites, which establish contact between each other by means of the N-terminal α-a helices of each monomer (2). Nevertheless, the persistence of the asymmetric spectral shift by stigmatellin in the bacterial enzyme even when the slow phase has disappeared (see Fig. 7) suggests that an even more rapid communication route for conformational changes might exist between center P sites in the dimer.

We conclude that the anti-cooperative QH_2 oxidation in the bc_1 complex dimer is a common feature of both prokaryotic and eukaryotic bc_1 complexes, helping to explain the conservation of the dimeric structure during evolution. Therefore, the same considerations we have discussed previously regarding the usefulness of such a mechanism in preventing electron leakage to oxygen at center P (6–8) apply to the relatively simpler 3-subunit bc_1 complex of bacteria. The asymmetric binding and catalysis at the center P sites whenever symmetry at center N is established, either by simultaneous vacancy or occupation with antimycin, further supports our previously proposed model (8) of regulatory interactions between substrate oxidation and reduction sites in the bc_1 complex dimer.

REFERENCES

1. Yang, X. H., and Trumpower, B. L. (1986) *J. Biol. Chem.* **261,** 12282–12289
2. Berry, E. A., Huang, L. S., Saechao, L. K., Pon, N. G., Valkova-Valchanova, M., and Daldal, F. (2004) *Photosynth. Res.* **81,** 251–275
3. Xia, D., Yu, C. A., Kim, H., Xian, J. Z., Kachurin, A. M., Zhang, L., Yu, L., and Deisenhofer, J. (1997) *Science* **277,** 60–66
4. Zhang, Z. L., Huang, L. S., Shulmeister, V. M., Chi, Y. I., Kim, K. K., Hung, L. W., Crofts, A. R., Berry, E. A., and Kim, S. H. (1998) *Nature* **392,** 677–684

5. Hunte, C., Koepke, J., Lange, C., Rossmanith, T., and Michel, H. (2000) *Structure Fold Des.* **8,** 669–684
6. Covian, R., Gutierrez-Cirlos, E. B., and Trumpower, B. L. (2004) *J. Biol. Chem.* **279,** 15040–15049
7. Covian, R., and Trumpower, B. L. (2005) *J. Biol. Chem.* **280,** 22732–22740
8. Covian, R., and Trumpower, B. L. (2006) *J. Biol. Chem.* **281,** 30925–30932
9. Trumpower, B. L., and Edwards, C. A. (1979) *J. Biol. Chem.* **254,** 8697–8706
10. Gutierrez-Cirlos, E. B., Merbitz-Zahradnik, T., and Trumpower, B. L. (2002) *J. Biol. Chem.* **277,** 1195–1202
11. Von Jagow, G., and Link, T. A. (1986) *Method Enzymol.* **126,** 253–271
12. Rich, P. R. (1984) *Biochim. Biophys. Acta* **768,** 53–79
13. Schröter, T., Hatzfeld, O. M., Gemeinhardt, S., Korn, M., Friedrich, T., Ludwig, B., and Link, T. A. (1998) *Eur. J. Biochem.* **255,** 100–106
14. Pfitzner, U., Odenwald, A., Ostermann, T., Weingard, L., Ludwig, B., and Richter, O. M. (1998) *J. Bioenerg. Biomembr.* **30,** 89–97
15. Korn, M. (1994) *Double Deletion of Cytochrome c Oxidase and Reductase (cta and fbc Operon) in Paracoccus denitrificans*, Ph.D. thesis, Johann Wolfgang Goethe-Universität, Frankfurt am Main, Germany
16. Anderka, O. (2005) *Structural and Functional Studies on the Cytochrome bc₁ Complex from Parococcus denitrificans*, Ph.D. thesis, Johann Wolfgang Goethe-Universität, Frankfurt am Main, Germany
17. Berden, J. A., and Slater, E. C. (1970) *Biochim. Biophys. Acta* **216,** 237–249
18. Snyder, C. H., and Trumpower, B. L. (1998) *Biochim. Biophys. Acta* **1365,** 125–134
19. Margoliash, E., and Walasek, O. F. (1967) *Method Enzymol.* **10,** 339–348
20. Kuzmic, P. (1996) *Anal. Biochem.* **237,** 260–273
21. Meinhardt, S. W., Yang, X., Trumpower, B. L., and Ohnishi, T. (1987) *J. Biol. Chem.* **262,** 8702–8706
22. Ritter, M., Anderka, O., Ludwig, B., Mäntele, W., and Hellwig, P. (2003) *Biochemistry* **42,** 12391–12399
23. Butler, J., Jayson, G. G., and Swallow, A. J. (1975) *Biochim. Biophys. Acta* **408,** 215–222
24. Sun, J., and Trumpower, B. L. (2003) *Arch. Biochem. Biophys.* **419,** 198–206
25. Muller, F. L., Roberts, A. G., Bowman, M. K., and Kramer, D. M. (2003) *Biochemistry* **42,** 6493–6499
26. Esser, L., Quinn, B., Li, Y. F., Zhang, M., Elberry, M., Yu, L., Yu, C. A., and Xia, D. (2004) *J. Mol. Biol.* **341,** 281–302
27. Von Jagow, G., and Ohnishi, T. (1985) *FEBS Lett.* **185,** 311–315
28. Ohnishi, T., Brandt, U., and von Jagow, G. (1988) *Eur. J. Biochem.* **176,** 385–389
29. Bowman, M. K., Berry, E. A., Roberts, A. G., and Kramer, D. M. (2004) *Biochemistry* **43,** 430–436
30. Berry, E. A., and Huang, L. S. (2003) *FEBS Lett.* **27,** 13–20
31. Covian, R., Pardo, J. P., and Moreno-Sanchez, R. (2002) *J. Biol. Chem.* **277,** 48449–48455
32. Wenz, T., Hellwig, P., Macmillan, F., Meunier, B., Trumpower, B. L., and Hunte, C. (2006) *Biochemistry* **45,** 9042–9052